Natural Resources Canada | Ressources naturelles Canada

GEOLOGICAL SURVEY OF CANADA
OPEN FILE 8946

Field relationships indicating cumulate intermingling at the Wrede Creek and Lunar Creek Alaskan-type ultramafic-mafic intrusions, north-central British Columbia

D. Milidragovic and N.R. Cleven

2023

Canada

ISSN 2816-7155
ISBN 978-0-660-47528-8
Catalogue No. M183-2/8946E-PDF

GEOLOGICAL SURVEY OF CANADA
OPEN FILE 8946

Field relationships indicating cumulate intermingling at the Wrede Creek and Lunar Creek Alaskan-type ultramafic-mafic intrusions, north-central British Columbia

D. Milidragovic and N.R. Cleven

2023

Permanent link: https://doi.org/10.4095/331430

This publication is available for free download through GEOSCAN (https://geoscan.nrcan.gc.ca/).

Recommended citation
Milidragovic, D. and Cleven, N.R., 2023. Field relationships indicating cumulate intermingling at the Wrede Creek and Lunar Creek Alaskan-type ultramafic-mafic intrusions, north-central British Columbia; Geological Survey of Canada, Open File 8946, 14 p. https://doi.org/10.4095/331430

Publications in this series have not been edited; they are released as submitted by the author.

Abstract

Convergent margin-related magmatic deposits hosted by ultramafic-mafic intrusions are becoming an increasingly important global resource of Ni-Cu-PGE. In the northern Canadian Cordillera, a sub-class of ultramafic-mafic intrusions, known as the Alaskan-type intrusions, are hosted within the accreted arc terranes of the North American continental margin. These intrusions have long been recognized for their chromite-associated PGE mineralization potential. However, their potential to host significant Ni-Cu-PGE sulfide mineralization and to be used in efforts to reduce greenhouse gas emissions through permanent carbon mineralization is becoming increasingly studied. This report describes the main lithologies and field relationships observed at the Wrede Creek and Lunar Creek Alaskan-type intrusions in British Columbia during recent fieldwork.

Introduction

Alaskan-type intrusions are deep-seated magmatic systems emplaced in convergent margin settings. Their potential to host critical metals (Pt ± Ir-subgroup of platinum group elements, or PGEs) in association with chromitite has been long recognized (e.g., Nixon et al. 1990, Johan 2002, Weiser 2002). These intrusive systems may also contain orthomagmatic sulfide mineralization with high tenors of critical metals: Ni, Cu, Rh, Pt, and Pd, as well as Au (e.g., Nixon et al. 2020, Milidragovic et al. 2021). Finally, the potential of Alaskan-type intrusions for long-term carbon mineralization (e.g., Voormeij and Simandl 2004, Mitchinson et al., 2020; Steinthorsdottir et al., 2022) remains largely unknown. Alaskan-type intrusions are especially abundant in the accreted Mesozoic arc terranes of the North American Cordillera (Fig. 1), with several large, well-exposed, and easily accessible intrusions located in British Columbia (e.g., Tulameen, Turnagain) and Alaska (e.g., Duke Island).

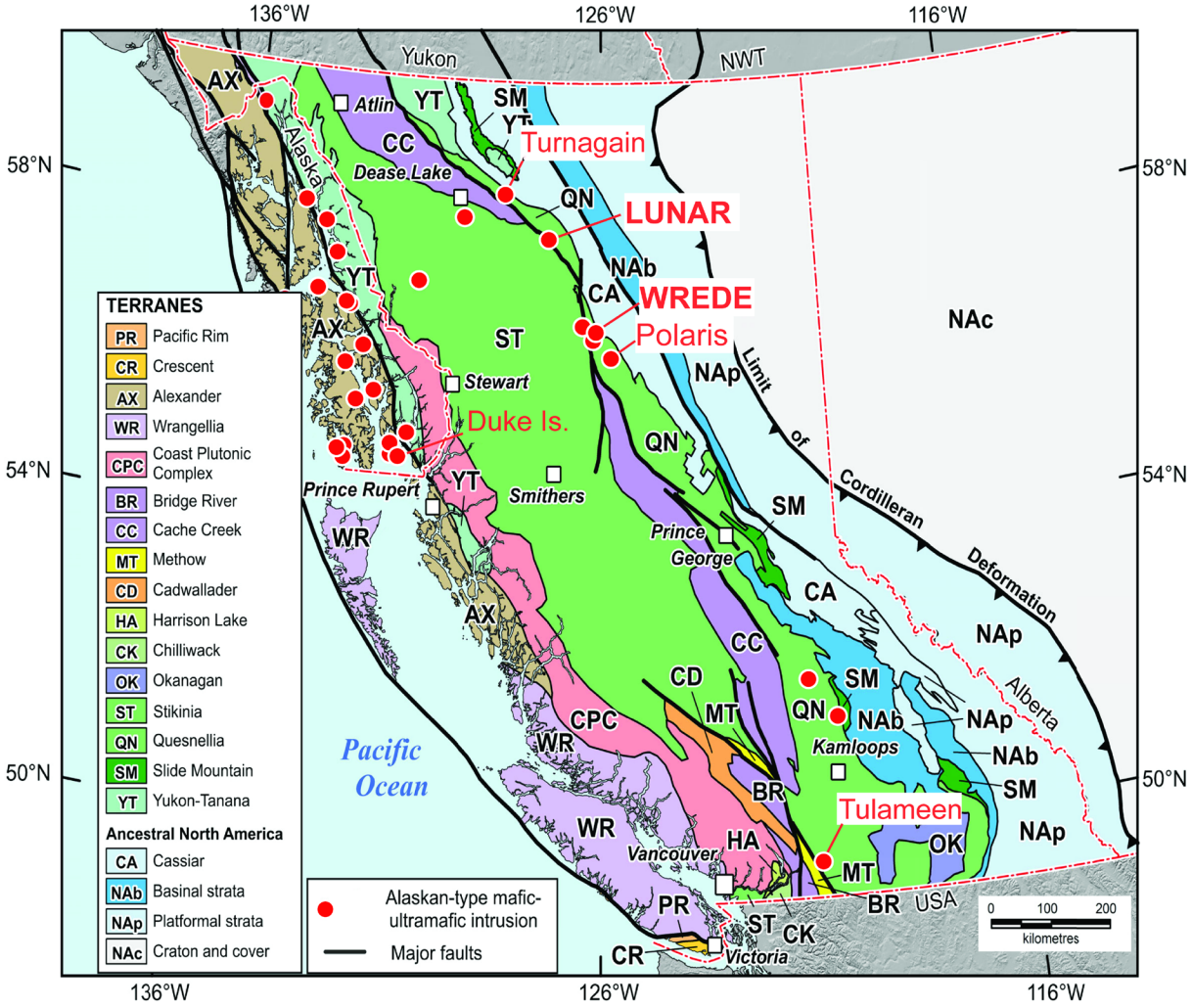

Figure 1. Terrane map of British Columbia and southeastern Alaska (after Colpron and Nelson 2011) showing the distribution of Alaskan-type intrusions (after Himmelberg and Loney 1995, Nixon et al. 1997). Modified from (Nixon et al. 2020).

The petrology and economic potential of Alaskan-type intrusions in the Canadian Cordillera remain largely speculative despite their well-documented potential for Ni-sulfide (e.g., Turnagain; ~1.8 Mt contained Ni at average grade of 0.21 % Ni; Mudd and Jowitt, 2014) and Pt-alloy mineralization (Tulameen; Nixon et al., 1990). Recent research has introduced a predictive petrological framework for mineralization in Alaskan-type intrusions (Milidragovic et al. 2021). To test this petrological framework, the existing geochemical database for Alaskan-type intrusions (Tulameen, Polaris, Turnagain, Duke Island) must be expanded, and targeted field study of intrusive field relationships is required. A two-week long field expedition to Wrede Creek and Lunar Creek Alaskan-type complexes (Fig. 1) was undertaken in August of 2022 in order to: 1) extend the existing collection of samples from Alaskan-type intrusions; 2) use the collected samples to acquire a high-quality geochemical dataset (major, trace, and noble elements) to be used in refining the petrological model for the genesis of Alaskan-type intrusions; and 3) to better understand the physical mechanisms by which Alaskan-type intrusions are emplaced. This report presents the preliminary interpretations of the intrusive relationships observed in the field.

Wrede Creek Complex

The Wrede Creek Alaskan-type mafic-ultramafic intrusion (Fig. 2) is located within the Ingenika Range of the Omineca Mountains, approximately 400 km north-northwest from Fort St. James (Fig. 1). Initial description of the Wrede Creek complex (Irvine 1974, 1976), was followed by 1:20,000 scale mapping and noble metal (Pt, Pd, Rh, Au) analysis by Nixon et al. (1997). The mapping and sampling reported here was limited to the southern half of the intrusion (Fig. 2).

The Wrede Creek complex extends over an area of ~10 km^2 and intrudes the subaqueous volcanic and volcaniclastic rocks of the Nicola (Takla) Group (Middle to Late Triassic) of the Quesnel terrane (Quesnellia; Fig. 2). The rocks of the Nicola Group are predominantly augite- and plagioclase-phyric crystal tuffs, flows, and volcanic breccia, metamorphosed at upper greenschist conditions (Nixon et al. 1997). In the immediate vicinity of the intrusion, the rocks of the Nicola Group are very fine-grained, extensively veined, and exhibit amphibolite-grade metamorphism (hornfels). Both the country rocks and the Wrede Creek complex are intruded by hornblende-bearing intermediate granitoids that may be as young as Middle Jurassic (Nixon et al. 1997).

The predominant lithology of the Wrede Creek complex is dunite (Figs. 2 and 3); however, detailed examination of outcrops in the southern part of the complex indicates that wehrlite also is present in significant abundance (Fig. 4A). Fine-grained crystals of chromite are ubiquitously disseminated in dunite; they are rarely concentrated into small irregular pods/schlieren of chromitite (Fig. 3A-B). Locally, dunite contains minor sulfides (Fig. 3C), as observed at field station 22MCD-21. Near-complete serpentinization of dunite is widespread, and is evidenced in

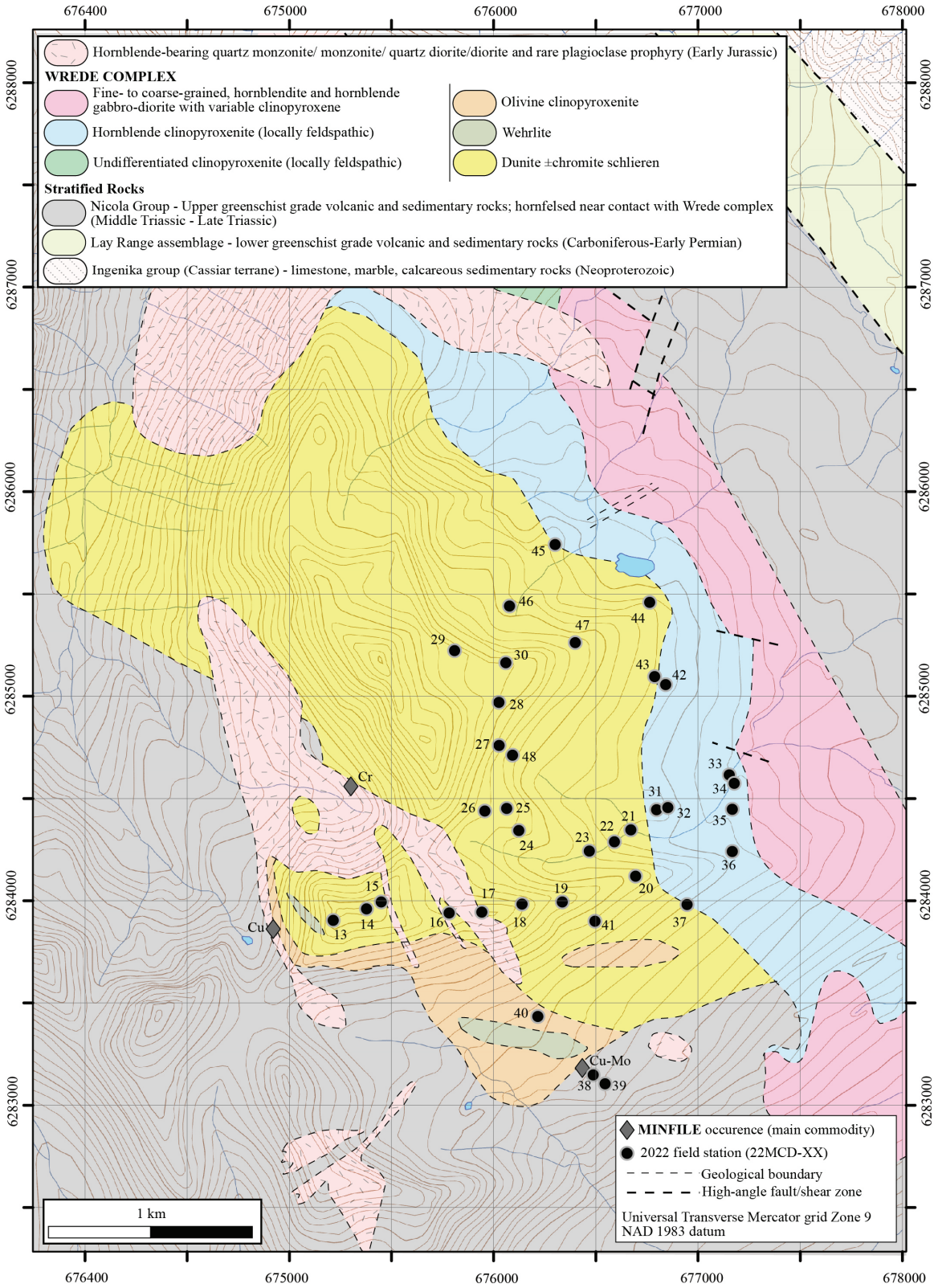

Figure 2. Simplified geology of the Wrede Creek complex, modified after Nixon et al. (1997).

Figure 3. Representative images of dunitic/wehrlitic rocks of the Wrede Creek complex. **A)** An irregular, cm-sized chromitite schlieren in a wehrlite, cross-cut by cm-wide veins of clinopyroxenite. Photograph by D. Milidragovic. NRCan photo 2022-473; **B)** Chromitite schlieren/layer in a strongly serpentinized dunite Photograph by D. Milidragovic. NRCan photo 2022-474; **C)** Very fine-grained disseminated sulfide in a pervasively serpentinized dunite. Photograph by D. Milidragovic. NRCan photo 2022-475; **D)** Orange weathering zone of listvenite within strongly serpentinized dunite/wehrlite. Photograph by. D. Milidragovic. NRCan photo 2022-476; **E)** Hand sample of listvenite containing abundant green fuchsite. Photograph by N. Cleven. NRCan photo 2022-477; **F)** A corridor of listvenite alteration cross-cutting serpentinite. Photograph by D. Milidragovic. NRCan photo 2022-478. Field station number, where applicable, is shown in the top right corner of each photograph.

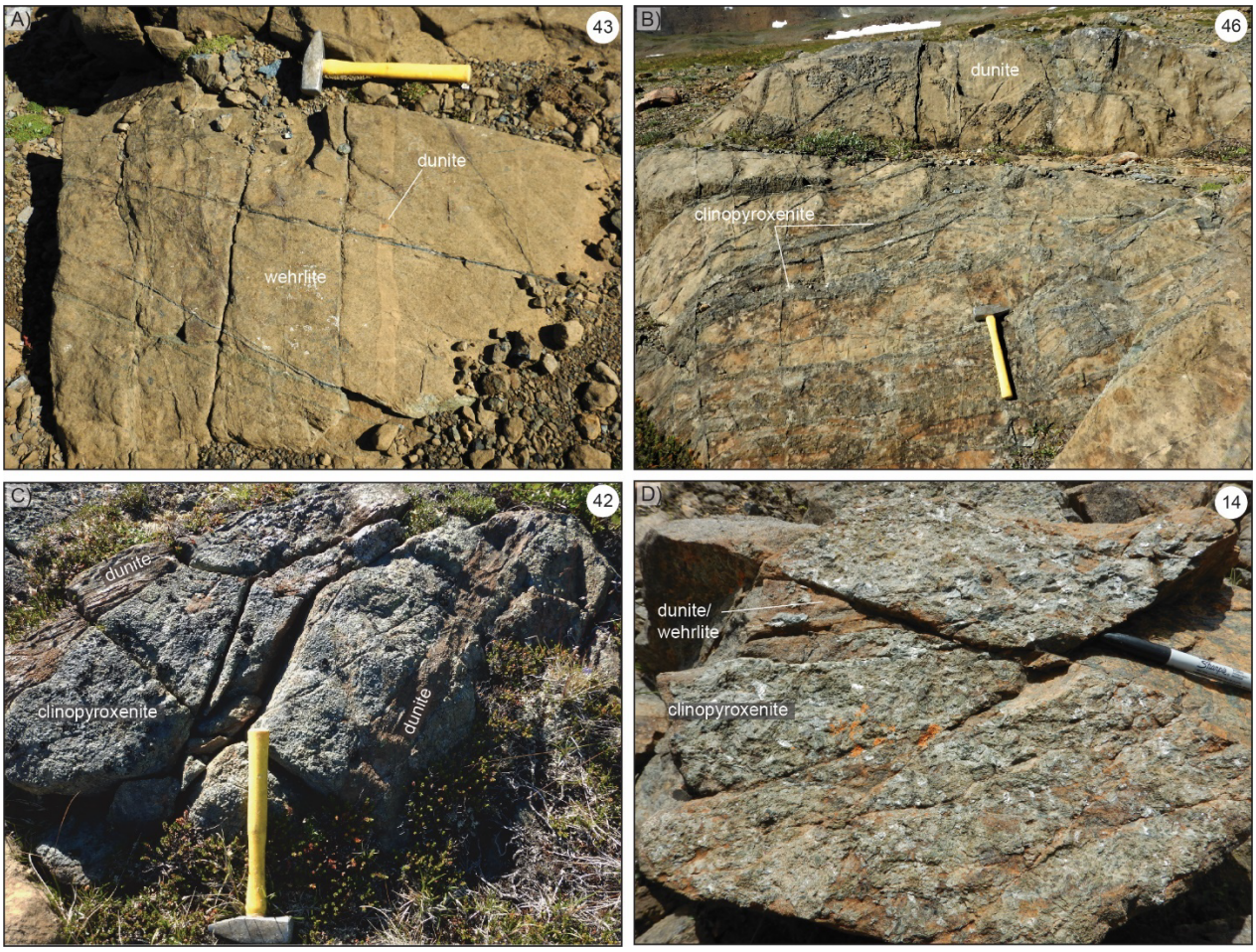

Figure 4. Representative images of field relationships among lithologies of the Wrede Creek complex. **A)** A dun-coloured, monomineralic, tabular dunite dike ~6 cm wide, cross-cutting a yellow-brown weathering wehrlite. Contrasts in weathering, such as observed here, aid in accurate identification of rock-types. Photograph by D. Milidragovic. NRCan photo 2022-479; **B)** Dunite cross-cut by several generations of clinopyroxenite dikes. Clinopyroxenite dikes range from sharp and tabular to irregular and undulose and with more diffuse boundaries. Photograph by D. Milidragovic. NRCan photo 2022-480; **C)** Grey-green clinopyroxenite crosscut, by irregular, brown, strongly foliated septa of serpentinized dunite/wehrlite. Photograph by D. Milidragovic. NRCan photo 2022-481; **D)** Pegmatitic green clinopyroxenite, containing brown-weathering olivine-rich "pockets" of dunite/wehrlite. Photograph by N. Cleven. NRCan photo 2022-482. Field station number, where applicable, is shown in the top right corner of each photograph.

weathered outcrop faces by macroscopic mesh textures around black serpentine pseudomorphs after olivine (Fig. 3B), and serpentine selvedges around veins and apparent hydrothermal fluid conduits.

Extensive carbonate alteration of serpentinized dunite forming yellow/orange-weathering, foliated listvenite (Fig. 3D-E; magnesite + quartz + talc + fuchsite; e.g., Cutts et al. 2021), is locally significant and concentrated along brittle faults and fracture zones (Fig. 3F). Clinopyroxenite is a subordinate lithology in the Wrede Creek complex, and it includes the full spectrum between olivine-rich and hornblende-rich phases (Nixon et al. 1997). Olivine clinopyroxenite largely occurs in the southwestern part of the intrusion where it is

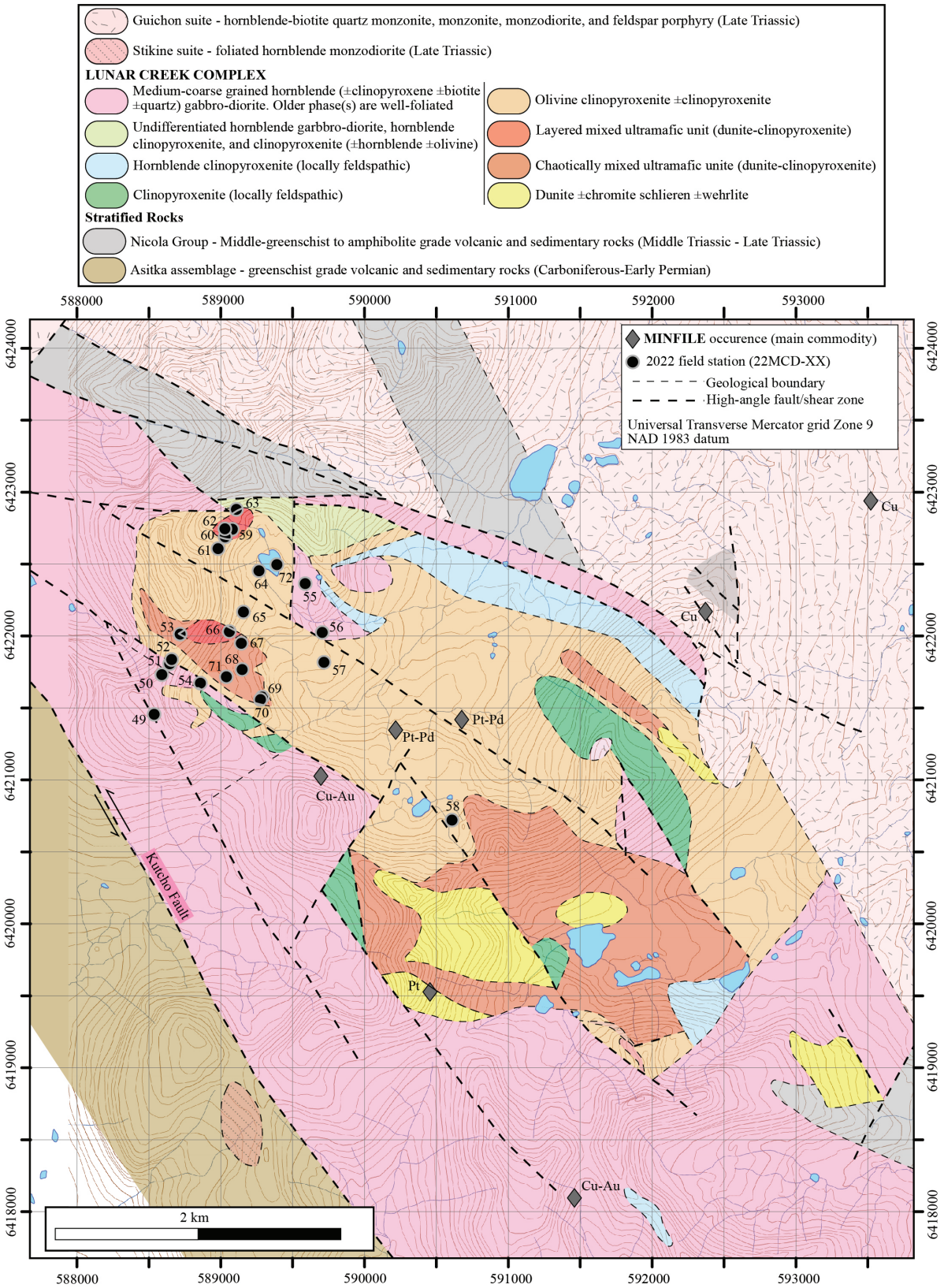

Figure 5. Simplified geology of the Lunar Creek complex, modified after Nixon et al. (1997).

densely cross-cut by thin (1-5 cm) dikes of clinopyroxenite. Clinopyroxenite in the eastern part of the complex is highly heterogeneous and varies from medium- to very coarse-grained. The contact between the dunite core and clinopyroxenite to the west shows, both, multiple generations of clinopyroxenite dikes intruded into dunite (Fig. 4B), and intrusion of strongly foliated dunite into clinopyroxenite (Fig. 4C). The easternmost portion of the complex is poorly exposed but is inferred from sparse outcrop observations to comprise heterogeneous gabbro-diorite containing variable proportions of hornblende, plagioclase, and clinopyroxene, overprinted by epidote alteration. A medium-grained, isotropic diorite at station 22MCD-33 was observed to contain trace amounts of disseminated chalcopyrite/pyrite and prominent malachite staining.

Lunar Creek Complex

The Lunar Creek Alaskan-type mafic-ultramafic complex (Fig. 5) is located within the Stikine Range of the Omineca Mountains, approximately 155 km east-southeast from Dease Lake (Fig. 1). The intrusion was first reported by Gabrielse and Dodds (1974) and Irvine (1976), and subsequently described in detail by Nixon et al. (1997). In addition to producing a 1:20,000 scale geological map, Nixon et al. (1997) reported a Middle Triassic minimum crystallization age for the complex (237 ±2 Ma; zircon U-Pb TIMS age from a equigranular hornblende diorite) and 84 PGE + Au analyses of representative samples from both the intrusive complex and the surrounding rocks. The mapping and sampling reported here was limited to the northwestern part of the intrusion (Fig. 5).

The Lunar Creek complex is exposed east of the Kutcho Fault within Quesnellia. The Kutcho fault is a major strike-slip fault that, at the latitude of the complex, separates Quesnellia from the Paleozoic basement rocks of the Stikine terrane (Stikinia). The ultramafic portion of the Lunar Creek complex is exposed across a broadly elliptical (7 km x 3 km) area; the extent of the entire

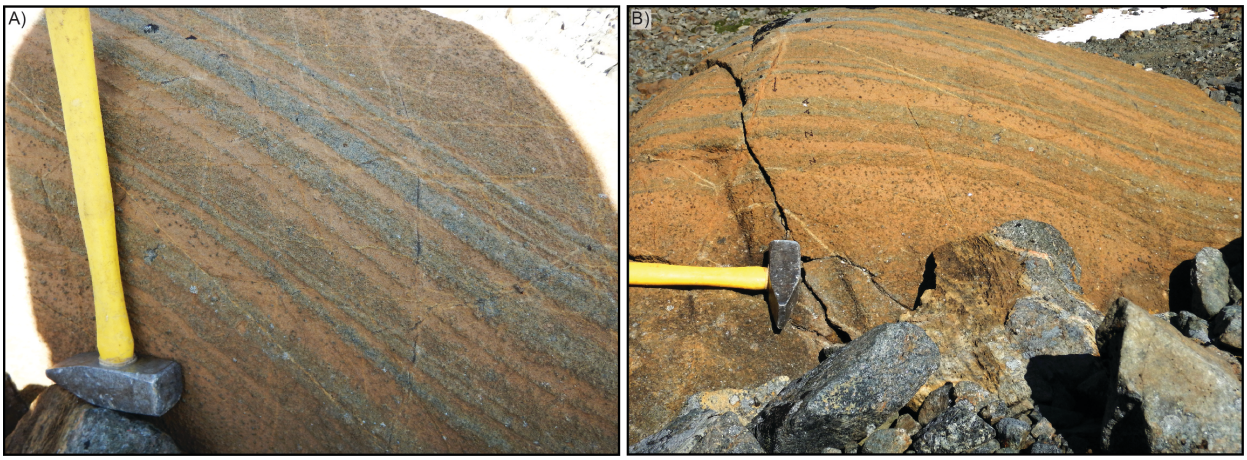

Figure 6. **A-B)** Centimetre-scale magmatic layering in ultramafic rocks of the Lunar Creek Complex, comprising dunite, wehrlite and olivine clinopyroxenite. Brown-weathering layers are olivine rich, green and grey-weathering layers are clinopyroxene rich. Photographs by D. Milidragovic. NRCan photos 2022-483 and 2022-484.

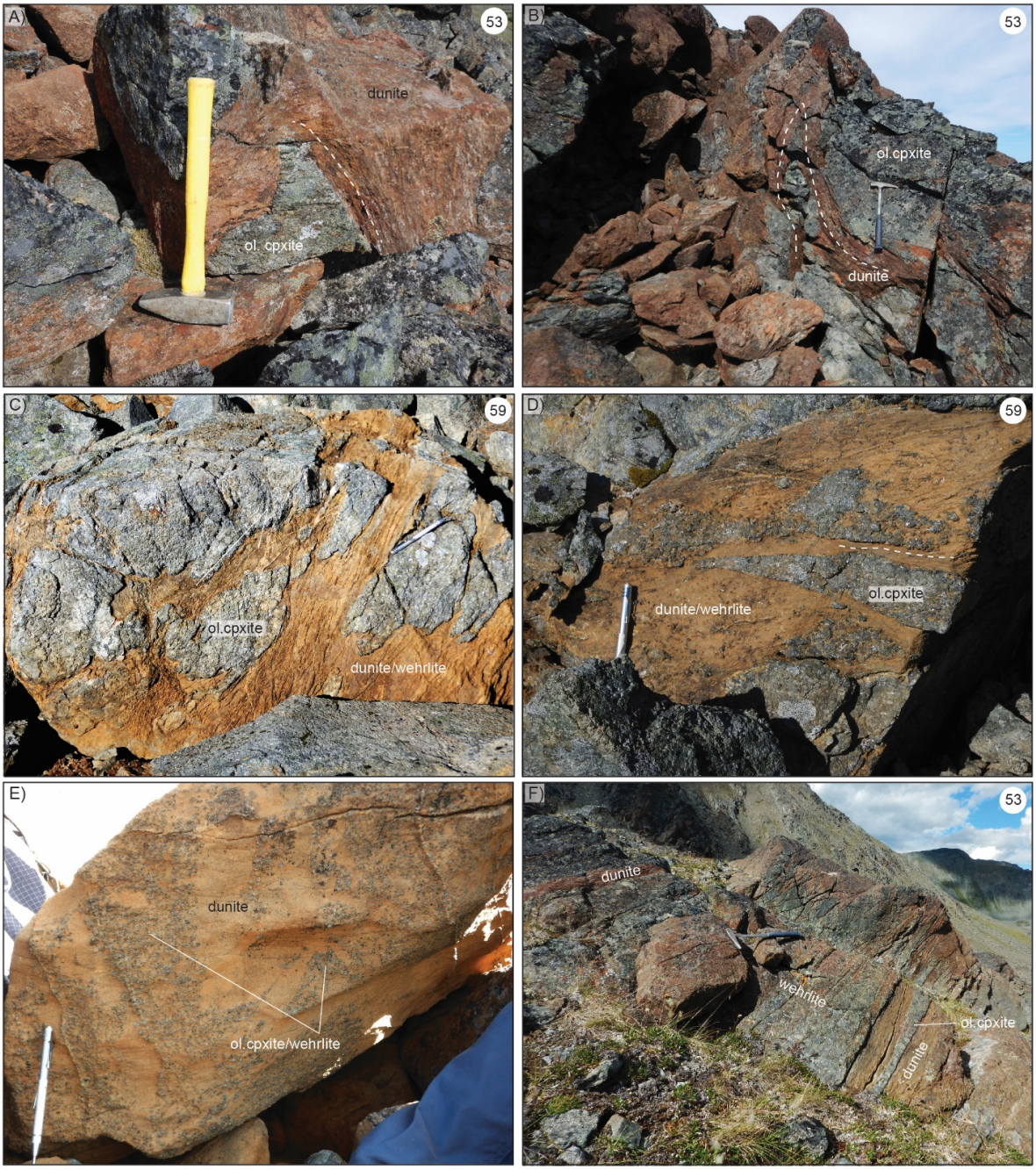

Figure 7. Field relationships among ultramafic lithologies of the Lunar Creek complex. **A)** Angular block of olivine clinopyroxenite completely engulfed by strongly foliated serpentinized dunite (or wehrlite). Photograph by D. Milidragovic. NRCan photo 2022-485; **B)** Septum of foliated serpentinized dunite intruded into olivine clinopyroxenite. Photograph by D. Milidragovic. NRCan photo 2022-486; **C-D)** Angular blocks of olivine clinopyroxenite, showing various extents of mechanical disaggregation, in a foliated serpentinized dunite matrix. Photographs by D. Milidragovic. NRCan photos 2022-487 and 2022-488; **E)** Heterogeneous ultramafic boulder, comprising irregular cm-size domains of dunite and variably disaggregated olivine clinopyroxenite. Photograph by D. Milidragovic. NRCan photo 2022-489; **F)** Sub-parallel layers of olivine clinopyroxenite, wehrlite, and foliated serpentinized dunite. Contacts between "layers" vary from sharp to irregular to diffuse. Layers vary in thickness and are discontinuous on m-scale (e.g., olivine clinopyroxenite on the right-hand side of the photo). Photograph by N. Cleven. NRCan photo 2022-490.

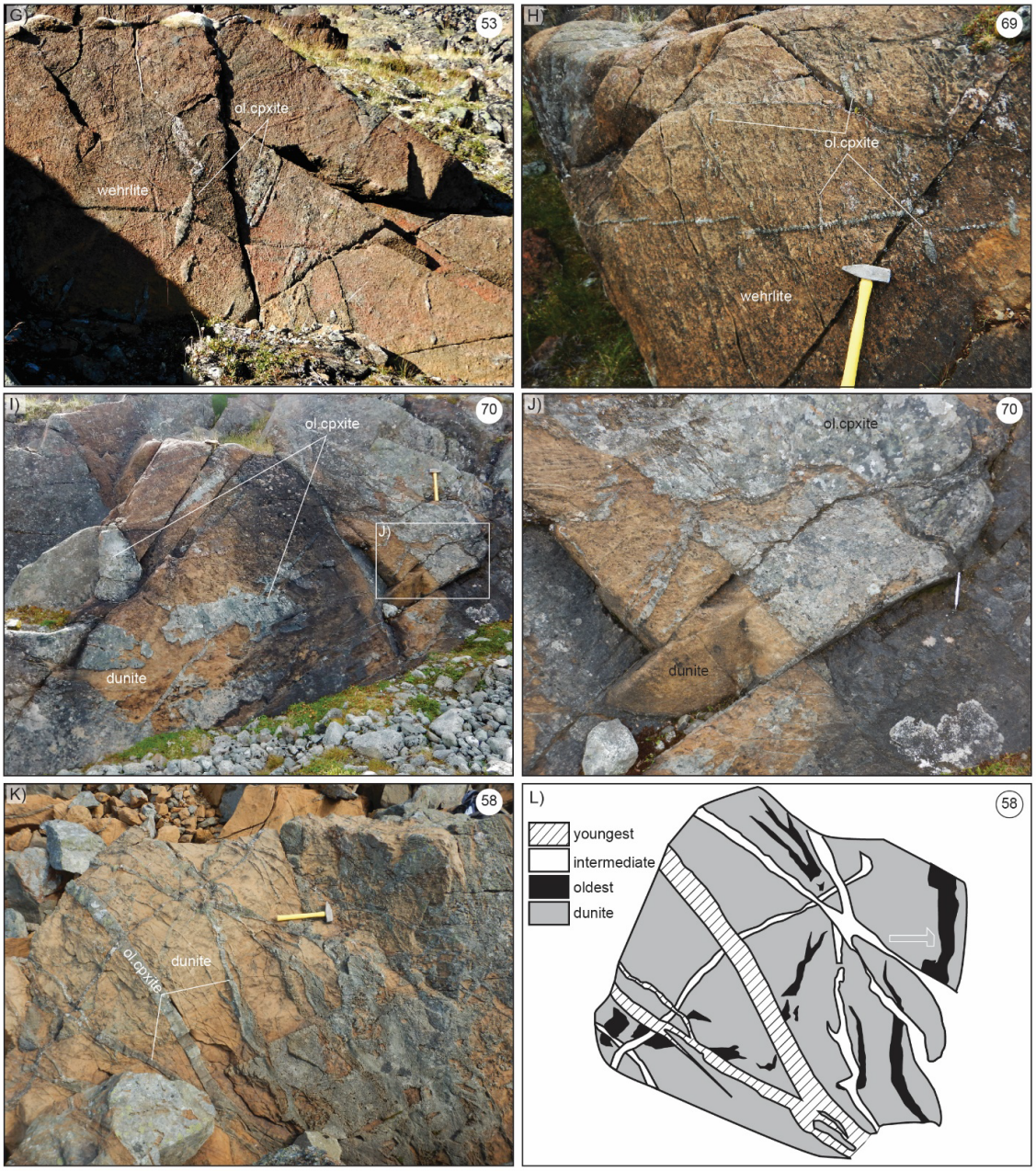

Figure 7. cont. G) Aligned boudins of clinopyroxenite in wehrlite. Photograph by D. Milidragovic. NRCan photo 2022-491; **H)** pencil-shaped aligned boudins of clinopyroxenite in wehrlite. A late vein of clinoproxenite, offset by a brittle fault, is perpendicular to the dominant fabric. Photograph by D. Milidragovic. NRCan photo 2022-492; **I)** An irregular, massive body of dunite intruding olivine clinopyroxenite. Angular blocks of olivine clinopyroxenite are seen stoping into dunite on the right-hand side of the photo. Photograph by N. Cleven. NRCan photo 2022-493; **J)** An expanded view (see Fig. 6I) of a foliated septum of dunite infilling the void generated by stoped olivine clinopyroxenite. The foliated dunite septum shows no evidence of crystallized trapped melt at its pointy termination. Photograph by D. Milidragovic. NRCan photo 2022-494; **K)** A large (~10 m-size) boulder of dunite cut by at least three generations of olivine clinopyroxenite. Photograph by N. Cleven. NRCan photo 2022-495; **L)** Schematic illustration of crosscutting relationships in K). Oldest dikes are strongly boudinaged, commonly have diffuse boundaries, and are cross-cut by younger pyroxenite dikes. Youngest dikes show minor deformation and have sharp boundaries. Field station number, where applicable, is shown in the top right corner of each photograph. Abberviations: ol. cpxite -olivine clinopyroxenite.

intrusion, including the gabbro-dioritic components, is ~14 km x 4 km. The long axis of the intrusion parallels the regional NW-SE tectonic grain. Along its eastern margin, the Lunar Creek complex is in structural contact with foliated, greenschist- to lower amphibolite-facies, augite-phyric, volcanic rocks of the Middle-Late Triassic Nicola (Takla) Group (Nixon et al. 1997). The contact between the rocks of the Nicola Group and the Lunar Creek complex is a locally mylonitic ductile shear zone. Both the Lunar Creek complex and the Nicola Group volcanic rocks are intruded by granitoids, including plagioclase porphyry dikes, of the Pitman batholith, part of the Late Triassic Guichon suite (Mortimer et al. 1990, Woodsworth et al. 1991).

The Lunar Creek complex comprises all of the lithologies characteristic of Alaskan-type intrusions, including dunite (±chromitite), wehrlite, olivine clinopyroxenite, (hornblende) clinopyroxenite, and gabbro-diorite (Irvine 1976, Nixon et al. 1997). In contrast to the Wrede Creek complex, the abundance of dunite exposed at the surface at the Lunar Creek complex is low, and chromitite schlieren are uncommon. Notably, serpentinized dunite sometimes displays pale weathering and extensive magnetite veining, indicative of locally significant iron mobility (c.f., Steinthorsdottir et al. 2022). Nixon et al. (1997) reported at least two generations of gabbro-diorite: an older foliated phase, and a younger volumetrically-dominant equigranular phase whose ca. 237 Ma age provides the minimum age of the intrusion.

Rare compositionally layered boulders in the northernmost part of the intrusion suggest limited preservation of syn-crystallization injection, or primary magmatic interlayering textures (Fig. 6). However, expansive zones of spectacular, chaotic, mixed or hybridized ultramafic cumulates that grade between dunite and olivine clinopyroxenite (Figs. 7 and 8), as described below indicate that much of the Lunar Creek complex experienced late, near-solidus remobilization.

The chaotically mixed ultramafic rocks of the Lunar Creek complex

The chaotically mixed rocks are widespread in the northwestern part of the intrusion. They are generally characterized by irregular, straight to lobate contacts between ultramafic rock types, with common rafts of one type within another; these rafts can exhibit varying degrees of resorption within the encompassing lithology (Fig. 7E). Dyke- or sill-like structures are common; however, they are not laterally continuous (Fig. 7F), and can pinch out or widen into amorphous bodies. As all phases involved are cumulate, these relationships are interpreted to reflect intermingling at near-solidus conditions. The two principal intermingled rock types are the variably serpentinized dunite and olivine clinopyroxenite. The related textures, described below, can appear on the cm- to m-scale. Rocks of identical appearance are also common at both Polaris (e.g., Nott et al. 2020) and Tulameeen (e.g., Spence et al. 2022) Alaskan-type intrusions (Fig.1).

The appearance of the intermingled cumulate rocks varies greatly and ranges from: 1) rocks composed predominantly of massive olivine clinopyroxenite intruded by foliated septa of strongly serpentinized (‘toothpaste’) dunite (Fig. 7A-B, see also Fig. 4C); through 2) rocks composed predominantly of wehrlite with angular blocks or pencil-shaped boudins of clinopyroxenite (Fig. 7C-D and 7G-H); and 3) rocks composed predominatly of dunite, successively intruded

by several generations of discrete clinopyroxenite dikes, with the earliest generations exhibiting boudinage, or disaggregation, and a degree of mineral resorption (Fig. 7K-L). Clinopyroxenite commonly shows strong evidence of mechanical disaggregation, especially within rafts and at mingled lithological contacts with dunite (Fig. 7C-D, and Fig. 7I-J). Extreme degrees of disaggregation and homogenization likely result in hybrid, mechanically produced wehrlites, such as those in Fig. 7G-H. Conversely, some coarse-grained olivine clinopyroxenites show evidence of progressive disaggregation of dunite septa (Fig. 8), and may also be interpreted as hybrids formed by intermingling.

Our field observations allow for several key inferences to be made:

- Magma injection (and mixing) was likely episodic, as indicated by several generations of diking in Fig. 6K-L. A variety of dynamic processes, including magmatic recharge, large earthquakes, and gravitational slumping, may have resulted in the observed magmatic disruption
- Typically, olivine clinopyroxenite is massive and shows evidence of brittle disaggregation and boudinage during mixing with less viscous dunite. This suggests that dunite was generally the less competent lithology at relatively high temperatures of deformation (>800ºC; e.g., Herwegh et al. 2011, Linckens et al. 2011).

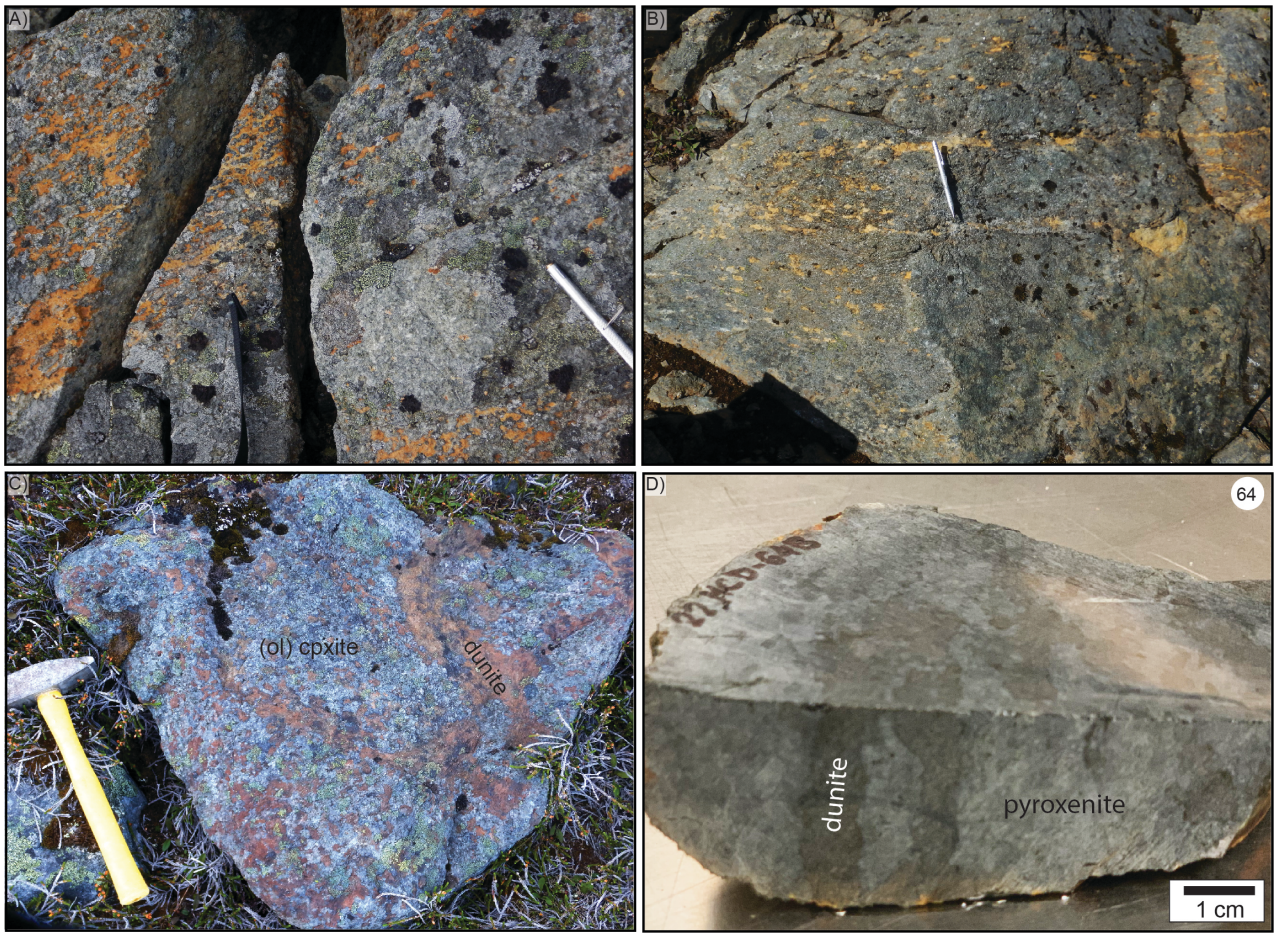

Figure 8. Hybrid olivine clinopyroxenites of the Lunar Creek complex. **A-C)** Field relations illustrating spatial association between thin veins/septa of dunite intruding clinopyroxenite and coarse-grained, heterogeneous olivine clinopyroxenite. Photographs by D. Milidragovic. NRCan photos 2022-496, 2022-497, and 2022-498; **D)** three-dimensional view of aligned cm-scale dunitic septa in a hybrid olivine clinopyroxenite. Photograph by D. Milidragovic. NRCan photo 2022-499.

- Similar field relationships exist at the Wrede Creek complex and have been documented at other Cordilleran Alaskan-type intrusions (Nott et al. 2020, Spence et al. 2022).
- The observation that some patchy, coarse-grained olivine clinopyroxenites are hybrids formed by mechanical disaggregation of dunite indicates that in some cases dunite was the rheologically more competent lithology. This behaviour may be limited to situations where the volume fraction of dunite is relatively low, ceasing to form interconnected mechanically weak networks (Handy 1990, Herwegh et al. 2011).
- During intermingling, dunite was nearly free of interstitial melt (and formed ex-situ); the best evidence for this are the terminations of dunitic septae that pinch-out, but lack any evidence of crystallized trapped melt (e.g., late-stage crystallization of hornblende, plagioclase, or biotite).
- Wehrlite, in chaotically mixed rocks, is a mechanical mixture formed through advanced disaggregation of (olivine) clinopyroxenite during intermingling with near-solidus dunite and subsequent homogenization.

Future work

Future work will include:

1) Whole-rock geochemical analysis (major and trace element, PGE+Au, and volatile species) of ~100 samples from Wrede Creek and Lunar Creek complexes.

2) In-situ analysis of chromite from both intrusions by electron probe microanalysis (EPMA) and laser ablation-inductively coupled plasma-mass spectrometry (LA-ICP-MS).

3) Submission of several coarse-grained, feldspathic samples for U-Pb zircon geochronology to better constrain the chronology of emplacement of both Wrede Creek and Lunar Creek complexes.

4) Physical property (magnetic susceptibility and density) and mineralogical analysis by X-ray diffraction (XRD) and thermogravimetric analysis (TGA) of serpentinites for the ongoing studies of carbon mineralization potential in the Canadian Cordillera.

Acknowledgments

We thank the Tsay Keh Dene and Kwadacha First Nations for being supportive of our fieldwork. Benchmark Metals and Apex Geoscience offered hospitality and logistical assistance at the Lawyers camp. We thank Silver King Helicopters for their flexibility and reliability. We thank S. Paradis for her thoughtful review, and J. Nott and G. Nixon for comments on an earlier version of this manuscript.

References:

Colpron, M., and Nelson, J.L. 2011. A digital atlas of terranes for the Northern Cordillera. British Columbia Ministry of Energy and Mines, British Columbia Geological Survey, Geofile **2011-11**.

Cutts, J.A., Steinthorsdottir, K., Turvey, C., Dipple, G.M., Enkin, R.J., and Peacock, S.M. 2021. Deducing Mineralogy of Serpentinized and Carbonated Ultramafic Rocks Using Physical Properties With Implications for Carbon Sequestration and Subduction Zone Dynamics. Geochemistry, Geophysics, Geosystems **22**, e2021GC009989, 23 p.

Gabrielse, H., and Dodds, C.J. 1974. Operation Finlay. Geological Survey of Canada, Paper **74-1A**, pp. 13–15.

Handy, M.R. 1990. The solid-state flow of polymineralic rocks. Journal of Geophysical Research **95**, 8647–8661.

Herwegh, M., Linckens, J., Ebert, A., Berger, A., and Brodhag, S.H. 2011. The role of second phases for controlling microstructural evolution in polymineralic rocks: A review. Journal of Structural Geology **33**, 1728–1750

Himmelberg, G.R., and Loney, R.A. 1995. Characteristics and petrogenesis of Alaskan-type ultramafic-mafic intrusions, southeastern Alaska. United States Geological Survey, Professional Paper **1564**, 47 p.

Irvine, T.N. 1974. Ultramafic and gabbroic rocks in the Aiken Lake and McConnell Creek map-areas,

British Columbia. Geological Survey of Canada, Paper **74**–**1A**, pp. 149–152.

Irvine, T.N. 1976. Studies of Cordilleran gabbroic and ultramafic intrusions, British Columbia. Geological Survey of Canada, Paper **76**–**1A**, pp. 75–81.

Johan, Z. 2002. Alaskan-type complexes and their Platinum-Group Element mineralization. *In* Geology, Geochemistry, Mineralogy and Mineral Beneficiation of Platinum-group Elements. *Edited by* L.J. Cabri. Canadian Institute of Mining and Metallurgy, Special Volume **54**, 669–719.

Linckens, J., Herwegh, M., Muntener, O., and Mercolli, I. 2011. Evolution of a polymineralic mantle shear zone and the role of second phases in the localization of deformation. Journal of Geophysical Research: Solid Earth **116**, 1–21.

Milidragovic, D., Nixon, G.T., Scoates, J.S., Nott, J.A., and Spence, D.W. 2021. Redox-controlled chalcophile element geochemistry of the Polaris Alaskan-type mafic-ultramafic complex, British Columbia, Canada. Canadian Mineralogist **59**, 1627–1661.

Mitchinson, D., Cutts, J., Fournier, D., Naylor, A., Dipple, G., Hart, C.J.R., Turvey, C., Rahimi, M., and Milidragovic, D. 2020. The carbon mineralization potential of ultramafic rocks in British Columbia: a preliminary assessment. Geoscience BC Report **2020-15**/MDRU Publication **452**, 25 p.

Mortimer, N., van der Heyden, P., Armstrong, R.L., and Harakal, J. 1990. U-Pb and K-Ar dates related to the timing of magmatism and deformation in the Cache Creek terrane and Quesnellia, southern British Columbia. Canadian Journal of Earth Science **27**, 117–124.

Nixon, G.T., Cabri, L.J., & Laflamme, J.H.G. 1990. Platinum-group-element mineralization in lode and placer deposits associated with the Tulameen Alaskan-type complex, British Columbia. Canadian Mineralogist **28**, 503–535.

Nixon, G.T., Hammack, J.L., Ash, C.H., Cabri, L.J., Case, G., Connelly, J.N., Heaman, L.M., Laflamme, J.H.G., Nuttall, C., Paterson, W.P.E., and Wong, R.H. 1997. Geology and platinum group element mineralization of Alaskan-type ultramafic-mafic complexes in British Columbia. British Columbia Ministry of Employment and Investment, British Columbia Geological Survey Bulletin **93**, 142 p.

Nixon, G.T., Scoates, J.S., Milidragovic, D., Nott, J., Moerhuis, N., Ver Hoeve, T.J., Manor, M.J., and Kjarsgaard, I.M. 2020. Convergent margin Ni-Cu-PGE-Cr ore systems: U-Pb petrochronology and environments of Cu-PGE vs. Cr-PGE mineralization in Alaskan-type intrusions. Geological Survey of Canada, Open File **8722**, pp. 197–218.

Nott, J., Milidragovic, D., Nixon, G.T., and Scoates, J.S. 2020. New geological investigations of the Early Jurassic Polaris ultramafic-mafic Alaskan-type intrusion, north-central British Columbia. Geological Fieldwork 2019, British Columbia Ministry Of Energy, Mines, and Petroleum Resources, Paper **2020-01**, 59–76.

Spence, D.W., Crawford, H., Scoates, J.S., Nott, J.A., Nixon, G.T., and Milidragovic, D. 2022. Mapping ultramafic cumulates at the Tulameen ultramafic-mafic Alaskan-type intrusion, south-central British Columbia, aided by remotely piloted aircraft system photogrammetry. Geological Fieldwork 2021, British Columbia Ministry Of Energy, Mines and Low Carbon Innovation, Paper **2022-01**, 103–122.

Steinthorsdottir, K., Dipple, G.M., Cutts, J.A., Turvey, C.C., Milidragovic, D., and Peacock, S.M. 2022. Formation and preservation of brucite and awaruite in serpentinized and tectonized mantle in central British Columbia: implications for carbon mineralization and nickel mining. Journal of Petrology **63**, 1-25.

Voormeij, D. A. and Simandl, G. J. 2004. Geological, ocean, and mineral CO_2 sequestration options: a technical review. Geoscience Canada 31, 11–22.

Weiser, T.W. 2002. Platinum-group minerals (PGM) in placer deposits. *In* The Geology, Geochemistry, Mineralogy and Mineral Beneficiation of Platinum-group Elements. *Edited by* L.J. Cabri. Canadian Institute of Mining and Metallurgy, Special Volume **54**, 721–756.

Woodsworth, G.J., Anderson, R.G., Armstrong, R.L., Struik, L.C., and van der Heyden, P. 1991. Chapter 15: Plutonic Regimes. *In* Geology of the Cordilleran Orogen in Canada. *Edited by* H. Gabrielse and C.J. Yorath. Geological Survey of Canada, Geology of Canada, No. **4**. pp. 491–531.